Cell, Vol. 101, 635–645, June 9, 2000, Copyright ©2000 by Cell Press

Chromosome Missegregation and Apoptosis in Mice Lacking the Mitotic Checkpoint Protein Mad2

Max Dobles,* Vasco Liberal,†‖ Martin L. Scott,*§ Robert Benezra,† and Peter K. Sorger*‡
*Department of Biology
Massachusetts Institute of Technology
Cambridge, Massachusetts 02139
†Department of Cell Biology
Sloan Kettering Memorial Cancer Center
New York, New York 10021

Summary

The initiation of chromosome segregation at anaphase is linked by the spindle assembly checkpoint to the completion of chromosome–microtubule attachment during metaphase. To determine the function of the mitotic checkpoint protein Mad2 during normal cell division and when mitosis goes awry, we have knocked out *Mad2* in mice. We find that E5.5 embryonic cells lacking *Mad2*, like *mad2* yeast, grow normally but are unable to arrest in response to spindle disruption. At E6.5, the cells of the epiblast begin rapid cell division and the absence of a checkpoint results in widespread chromosome missegregation and apoptosis. In contrast, the postmitotic trophoblast giant cells survive without *Mad2*. Thus, the spindle assembly checkpoint is required for accurate chromosome segregation in mitotic mouse cells, and for embryonic viability, even in the absence of spindle damage.

Introduction

During mitosis, chromosomes are segregated with high fidelity. In *S. cerevisiae*, for example, the frequency of chromosome nondisjunction is only about 1×10^{-5} per cell division (Hartwell et al., 1982). This remarkable fidelity depends both on the intrinsic accuracy of the segregation machinery and on the operation of the spindle assembly checkpoint. The spindle checkpoint is a highly conserved signal transduction pathway that links the initiation of anaphase to spindle assembly and the completion of chromosome–microtubule attachment (Hoyt et al., 1991; Li and Murray, 1991; Li and Benezra, 1996; Taylor and McKeon, 1997). The presence of even a single misaligned or unattached chromosome is sufficient to activate the checkpoint, inhibit the anaphase promoting complex (APC), and arrest a cell at the metaphase to anaphase transition (Rieder et al., 1994; Li and Nicklas, 1995; Li et al., 1997; Hwang et al., 1998; Kim et al., 1998). Arrest caused by an unattached chromosome is overcome by laser ablation of the kinetochore, the structure that mediates chromosome–microtubule attachment (Rieder et al., 1995). Thus, the signal for checkpoint-dependent arrest arises from, or is transduced through, kinetochores.

Genes involved in the spindle assembly checkpoint were first identified in the yeast *S. cerevisiae* and include the mitotic arrest defective genes *MAD*1–3 (Li and Murray, 1991) and the budding uninhibited by benzimidazole genes *BUB*1–3 (Hoyt et al., 1991). Mad1–3p, Bub1p, and Bub3p are proteins that link anaphase to the completion of spindle assembly (Hardwick et al., 1996; Alexandru et al., 1999), but Bub2p appears to be part of a second pathway that acts later in the cell cycle to link spindle assembly to mitotic exit and cytokinesis (Alexandru et al., 1999; Clute and Pines, 1999; Fraschini et al., 1999; Li, 1999). All six of these genes are dispensable for normal growth, apparently because mitosis in *S. cerevisiae* lasts long enough for all chromosomes to attach to the spindle before anaphase begins, even in the absence of a checkpoint. The addition of antimicrotubule drugs to yeast cells lacking any single *MAD* or *BUB* gene causes the cells to proceed through mitosis without having established chromosome–microtubule attachments. This causes extensive chromosome loss and cell death (Hoyt et al., 1991; Li and Murray, 1991).

Homologs of the yeast checkpoint genes have been cloned from animal cells (Li and Benezra, 1996; Taylor and McKeon, 1997; Chan et al., 1998; Jin et al., 1998; Taylor et al., 1998). Genetic analysis of these genes has just begun, but *C. elegans mad1* (Kitagawa and Rose, 1999) and *Drosophila bub1* (Basu et al., 1999) are essential genes whose mutation causes aberrant chromosome segregation. It is not yet known why spindle checkpoint genes are dispensable in budding and fission yeast but essential in worms and flies. One important difference between yeast and metazoans is that only the later undergo apoptosis, an event that can be induced by chromosome damage (Woods et al., 1995; Jordan et al., 1996). The expression of a dominant-negative fragment of *BUB1* in human cells reduces nocodazole-dependent apoptosis (Taylor and McKeon, 1997), arguing that there is a specific connection between the spindle checkpoint and programmed cell death. One possibility is that apoptosis is triggered after a cell has experienced a prolonged mitotic arrest, thereby reducing the chance that the cell can escape the checkpoint and become aneuploid.

Biochemical, genetic, and cell biological experiments suggest that Mad and Bub proteins function as components of two closely linked pathways (Hardwick et al., 1996; Alexandru et al., 1999; Li, 1999). In animal cells, several Mad and Bub proteins localize to kinetochores unattached to microtubules, consistent with the observation that kinetochores are involved in generating the checkpoint signal (Li and Benezra, 1996; Taylor and McKeon, 1997; Chan et al., 1998; Jin et al., 1998; Martinez-Exposito et al., 1999). The recruitment of Mad2 to kinetochores involves an interaction with Mad1 (Chen et al., 1998, 1999; Jin et al., 1998). Mad2 also binds to

‡To whom correspondence should be addressed (e-mail: psorger@mit.edu).
§Present address: Biogen, Inc., 14 Cambridge Center, Cambridge, Massachusetts 02142.
‖Contribution of the second author described in Acknowledgments.

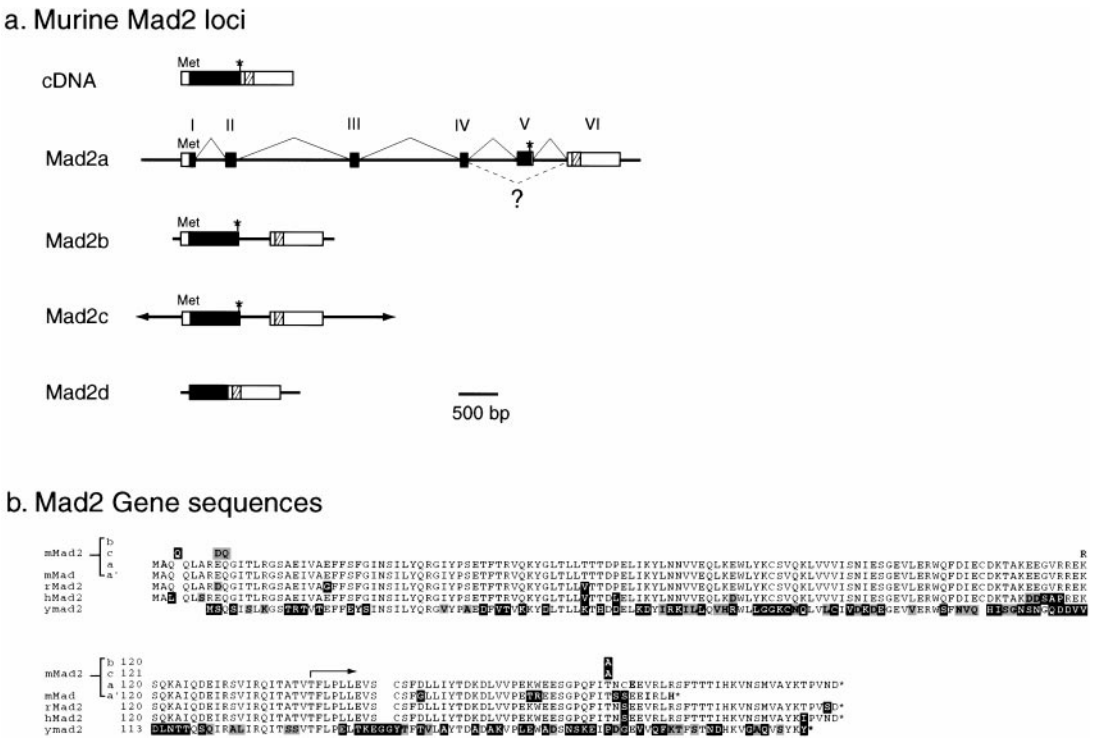

Figure 1. Structure of *Mad2* Genes in Mice

(A) Organization of the *Mad2* cDNA and of four distinct genomic loci. Regions homologous to the coding sequence of the cDNA are indicated (black boxes), as are the 5′ and 3′ UTRs (white boxes), and a potential alternatively spliced final coding region (hatched box). "Met" indicates the initiating methionine and asterisk (*) indicates the stop codon. *Mad2d* lacks an initiating methionine.

(B) Mad2 protein sequences determined from conceptual translations of the mouse genomic loci *Mad2a–c*, rat (r*Mad2*), human (h*Mad2*) and yeast (y*MAD2*) cDNAs. Gray boxes indicate conserved changes and black boxes indicate differences relative to mMad2a. Mouse Mad2a is 40% identical in protein sequence to yeast Mad2p and 95% identical to human Mad2. Mad2a′ denotes the protein that could be produced by splicing exon IV to exon VI, skipping exon V. This alternative splicing has not been observed to occur in isolated cDNAs. The sequences of mMad2b and c are shown only where they differ from that of mMad2a. The arrow marks the primer used to sequence polymorphic regions of cDNA clones. Complete sequences of Mad2a–d have been deposited in GenBank; accession numbers AF261919, AF261920, AF261921, and AF259902.

Cdc20 (Li et al., 1997; Fang et al., 1998; Hwang et al., 1998; Kim et al., 1998; Wassmann and Benezra, 1998), an essential activator of the APC (Visintin et al., 1997; Shirayama et al., 1998), preventing APC activation and stopping cell division at the metaphase to anaphase transition (Fang et al., 1998; Hwang et al., 1998; Kim et al., 1998; Wassmann and Benezra, 1998). Many molecular details remain to be worked out, but a reasonable model is that the activation of checkpoint kinases such as Bub1 promotes the formation of Mad2p–Cdc20p–APC complexes, thereby inhibiting APC and preventing the degradation of proteins such as Pds1p (a regulator of sister chromatid cohesion), whose degradation is necessary for progression into anaphase (Cohen-Fix et al., 1996; Yamamoto et al., 1996; Alexandru et al., 1999). However, alternative pathways have also been proposed (Chan et al., 1999; Hardwick et al., 2000).

To explore the function of the spindle assembly checkpoint in chromosome segregation, apoptosis, and genomic stability in mammalian cells, we have undertaken a genetic analysis of the murine *Mad2* checkpoint gene. We find that *Mad2* is essential and that *Mad2*$^{-/-}$ embryos die in utero about 6.5–7.5 days after conception (E6.5–E7.5). However, homozygous knockout embryos appear normal both in utero and in culture until embryonic day 5.5. *Mad2*$^{-/-}$ E5.5 cells are unable to arrest in mitosis in response to drug-induced spindle disruption, showing that they lack a functional spindle assembly checkpoint. The absence of this checkpoint allows *Mad2* null cells to proceed even when unattached chromosomes are present. This causes chromosomes to be missegregated and results in apoptotic cell death.

Results

Disrupting the Murine *Mad2* Gene

To isolate *Mad2* genomic DNA from mice, we probed strain 129/Sv libraries with ^{32}P-labeled rat or human *Mad2* cDNA (Li and Benezra, 1996). Restriction analysis and subsequent sequencing revealed four distinct *Mad2* genes (Figure 1A). Although *Mad2a–c* have the potential to encode full-length Mad2 (*Mad2d* lacks an initiating methionine), only *Mad2a* contains introns within the putative coding region. Two experiments were performed to test the idea that *Mad2a* is the only functional gene: (1) a murine embryonic cDNA library was probed with DNA sequences conserved among *Mad2a–c*, and (2) RT-PCR was performed on RNA from adult tissues. Sequencing of the *Mad2*-encoding cDNAs and RT-generated products showed that all *Mad2* mRNA was derived

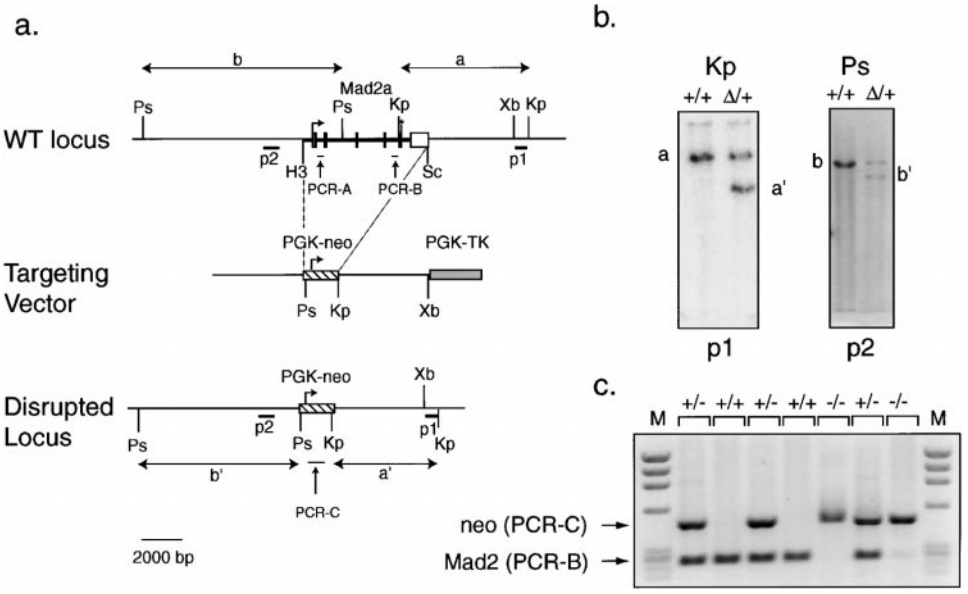

Figure 2. Disrupting the *Mad2a* Locus in ES Cells

(A) Structure of the wt *Mad2a* locus, the targeting vector, and the disrupted locus. The PGK-neomycin resistance cassette (hatched box) replaces *Mad2a* coding sequences (dark boxes) from the initiating methionine to the stop codon (asterisk). White boxes indicate 5′ and 3′ UTRs of the *Mad2* locus, and the gray box indicates a PGK-thymidine kinase cassette used for negative selection of ES cells. The restriction fragments used in the analysis of wt and targeted *Mad2a* loci are shown by arrows "a", "b", "a′", and "b′" and locations of Southern probes by "p1" and "p2." PCR-A, -B and -C indicate the PCR products used for genotyping (see Experimental Procedures for details). Diagnostic restriction sites are indicated as follows: Ps, PstI; Kp, KpnI; Sc, SacI; H3, HindIII, Xb, XbaI; additional sites for these enzymes are also present.

(B) Confirmation of *Mad2a* disruption in ES cells by Southern blotting following KpnI (Kp, probe p1) or PstI (Ps, p2) digestion. The origin of various bands is indicated with reference to the schematic (A).

(C) PCR genotyping of embryos grown in culture. Separate PCR reactions were performed to amplify the wt *Mad2* allele (PCR-B, see [A]) and the disrupted allele (PCR-C), and the samples then combined and analyzed on ethidium bromide–stained agarose gels. "M" indicates molecular weight markers.

from the *Mad2a* gene. We conclude that *Mad2a* is the functional *Mad2* locus and that *Mad2b–d* are pseudogenes. However, we cannot rule out completely the possibility that *Mad2b* and *c* are expressed in some tissues.

To disrupt *Mad2a* in ES cells, gene targeting was used to replace the entire *Mad2* coding region with a PGK-neomycin resistance cassette (Figure 2A). Cells from two independent 129/Sv-derived ES lines were injected into BL/6 blastocysts, and the resulting chimeras were backcrossed to BL/6 wild-type animals to generate lines 40 and 42. The structure of the disrupted *Mad2* locus was confirmed by Southern blotting and by PCR (Figures 2B and 2C).

Mad2 Is Essential for the Growth of Mitotic but Not Postmitotic Embryonic Cells

No homozygous null animals were observed in a total of 296 live births from *Mad2*$^{+/-}$ heterozygous intercrosses using either of the two founder lines (Table 1). Wild-type (wt) and heterozygous mice were born at the expected frequencies and appeared normal and healthy. Subtle differences in morbidity rates between age-matched colonies of *Mad2*$^{+/+}$ and *Mad2*$^{+/-}$ animals have been observed and histological analysis of some *Mad2*$^{+/-}$ animals reveals abnormalities of the spleen (increased germinal center formation) and a possible increase in tumor incidence. However, further analysis is required to determine the significance of these findings. We conclude that *Mad2* is an essential gene in mice and that *Mad2*$^{+/-}$ animals are largely normal.

To determine when *Mad2*$^{-/-}$ embryos die, we analyzed embryos from heterozygous intercrosses at various points of gestation. At E9.5–E13.5, none of 23 embryos examined were *Mad2* null. However, homozygous null embryos could be recovered during the blastocyst stage of development and then grown in culture (at E3.5, too early to establish fibroblast lines; Table 1). After 24–48 hr in culture, the spherical blastocysts flatten onto the culture dish and form a multicomponent structure in which the inner cell mass (ICM) grows as a mound on top of the extraembryonic (but embryonically derived) trophoblast cells (Figure 3). When *Mad2* null and wt embryos were cultured in vitro, they were observed to grow at similar rates through E5.5. However, the ICM of *Mad2* null embryos stopped proliferating after E6.5 and the cells began to die. Virtually no *Mad2*$^{-/-}$ ICM cells persisted to E8.5 (Figure 3).

In contrast, *Mad2*$^{-/-}$ trophoblast giant cells remained attached to the culture dish and continued to grow in size through E8.5 (the end of the experiment; Figure 3). The analysis of *Mad2* null trophoblast cells by phase contrast microscopy and BrdU labeling demonstrated that they were alive and undergoing DNA replication at E8.5 (data not shown), well past the point at which highly mitotic ICM cells die. Trophoblast giant cells are derived from cells that become mitotically inactive at about E4.5

Table 1. Viability Analysis of *Mad2*$^{-/-}$ Mice and Embryos

A. Genotypes of Live Births and Embryos from *Mad2*$^{+/-}$ Intercrosses

	Genotype				
	Mad2$^{+/+}$	*Mad2*$^{+/-}$	*Mad2*$^{-/-}$	ND[a]	Total
Live births, line 40	12	23	0		35
Live births, line 42	84	177	0		261
Embryos, E9.5–E13.5[b]	5	18	0		23
Blastocysts, E3.5[b]	20	31	7	9	67
Blastocysts grown in culture[b,c]					
Healthy at E8.5	5	11	0	0	16
ICM atrophied by E8.5	1	0	3	2	6

B. Histological Analysis of Embryos In Utero

		Number of Embryos			
Cross	Age	Total	Abnormal (A)	Resorbed (R)	Total (A+R)
Mad2$^{+/-}$ × *Mad2*$^{+/-}$	E6.0–E6.5	32	4	2	19%
Mad2$^{+/-}$ × *Mad2*$^{+/-}$	E6.5–E7.5	73	8	5	18%
Mad2$^{+/+}$ × *Mad2*$^{+/+}$	E6.5–E7.5	37	0	0	0%

Mice and E9.5–E13.5 embryos were genotyped either by Southern blotting KpnI-digested DNA (Figure 2) or by PCR of fragments PCR-A and C (see Figure 2). E3.5–E8.5 embryos were genotyped by amplification of regions PCR-B and C (see Figure 2). All embryos harvested at E3.5 were grown in culture to at least E5.5 before recovering DNA for genotyping.

For histological analysis embryos were fixed, sectioned, H&E stained, and scored as normal or abnormal based on size and general morphology. (Examples shown in Figure 4.) Empty decidua were scored as "Resorbed". Embryos from wild-type crosses were also examined as controls. TUNEL analysis was performed on 13 of the E6.5–E7.5 embryos from *Mad2*$^{+/-}$ intercrosses, and on 16 embryos from wt crosses. 3 embryos from *Mad2*$^{+/-}$ intercrosses, and none from wt crosses, were TUNEL positive (Figure 4).

[a] Not determined—genotyping was ambiguous.

[b] Derived from heterozygous intercrosses of Line 42.

[c] This represents typical data from one set of experiments. In related experiments, a total of 303 embryos were grown in culture. By E8.5, ICM cells atrophied in 5% (n = 95) of embryos from *Mad2*$^{+/-}$ × *Mad2*$^{+/+}$ crosses as compared to 17% (n = 208) from *Mad2*$^{+/-}$ intercrosses.

and undergo repeated rounds of S phase, generating a polyploid nucleus and a large cytoplasm (Rugh, 1990). We hypothesize that the survival of *Mad2*$^{-/-}$ trophoblast giant cells reflects a requirement for Mad2 specifically during mitosis.

Apoptosis in *Mad2* Null Embryos

When the gross morphologies of hematoxylin and eosin (H & E) stained embryos from *Mad2*$^{+/-}$ intercrosses were compared, no clear differences were seen at E5.5. By E6.5–E7.5, presumptive *Mad2*$^{-/-}$ embryos were considerably smaller than control littermates and were very disorganized (Figure 4 and Table 1). To investigate the cause of death in *Mad2*$^{-/-}$ embryos, we performed TUNEL on embryonic tissue sections. Embryos from wt animals appeared normal, with only a few apoptotic cells near the center of the embryo (Figure 4 and Table 1). About one-quarter of the embryos arising from heterozygous intercrosses exhibited a high incidence of TUNEL staining (Figure 4 and Table 1). Not all embryos from *Mad2*$^{+/-}$ intercrosses could be genotyped (see Figure 4 legend for details), but those Mad2$^{-/-}$ embryos whose genotypes could be determined had an abnormal gross morphology and were TUNEL positive. We conclude from these data that Mad2 null embryos undergo programmed cell death at E6.5–E7.5.

Despite the apparent restriction of the *Mad2* null phenotype to E6.5 and later, nullizygous embryos were recovered from heterozygous intercrosses at less than the Mendelian frequency of 25%. It seems unlikely that this is due to defects in gamete production, because *Mad2*$^{+/-}$ × wt crosses, in which the *Mad2*$^{+/-}$ parent was either the male or the female, yielded 50% *Mad2*$^{+/-}$ offspring (data not shown). Three measures of the frequency of *Mad2*$^{-/-}$ embryos among the progeny of *Mad2*$^{+/-}$ intercrosses (Table 1) imply that 30%–50% of *Mad2* null embryos die before implantation. We conclude that loss of *Mad2* causes some embryos to die prior to implantation (see Discussion), and the majority to undergo apoptotic death at about E6.5–E7.5.

Mad2 Is Required for Mitotic Arrest in Response to Spindle Disruption

Is Mad2 required for the mitotic checkpoint in mice as it is in yeast? The observation that *Mad2* null blastocysts grow normally in culture until E5.5 makes it possible to investigate this critical question. We treated cultured E5.5 embryos from heterozygous intercrosses with 2.5 μM nocodazole for 6 hr to disrupt spindle microtubules, disaggregated the embryos with trypsin, and then fixed cells onto coverslips for DAPI staining (Figures 5A–5D). The mitotic index of each embryo was determined by counting the fraction of cells with condensed chromosomes. A portion of the cells from each disaggregated embryo was reserved for genotyping by PCR. Whereas approximately 25% of the cells from *Mad2*$^{+/+}$ and *Mad2*$^{+/-}$ embryos contained condensed chromosomes, only 2% of the cells from *Mad2*$^{-/-}$ embryos were mitotic after nocodazole treatment. Thus, cells from *Mad2* null embryos do not arrest in mitosis in response to spindle disruption.

A potential caveat to the spindle depolymerization experiment is that *Mad2* null cells may fail to accumulate in mitosis simply because they are not actively cycling

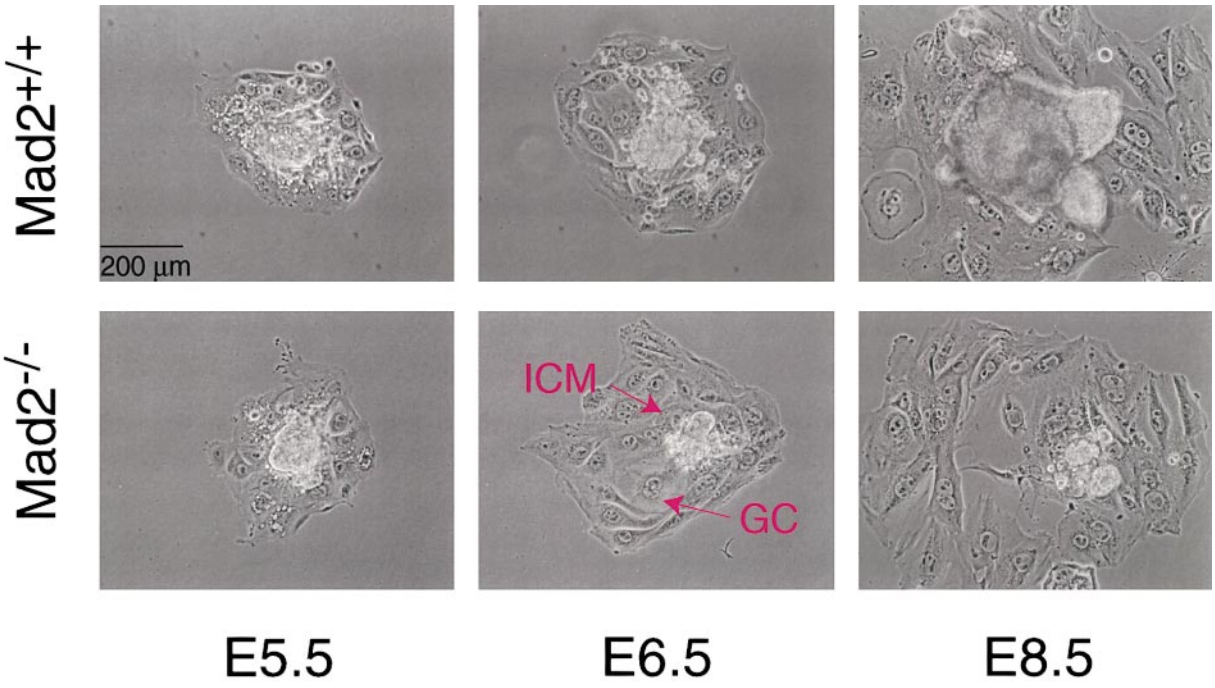

Figure 3. Growth of wt and *Mad2*$^{-/-}$ Embryos in Culture

Embryos grown in culture. E3.5 blastocysts from *Mad2* heterozygous intercrosses were cultured in vitro for 48 hr and then photographed using phase contrast microscopy. Arrows point to the inner cell mass (ICM) and to the trophoblast giant cells (GC). Photos were taken at E5.5, and then every 24 hr until E8.5. Genotypes were determined by PCR. Embryos exhibiting more extensive loss of ICM cells were common, but these embryos generally failed to yield PCR bands in the genotyping assay.

during the period of nocodazole treatment. To eliminate this possibility, we measured the fraction of cells in S phase by labeling with BrdU and the fraction in mitosis by staining for phosphorylated-Histone H3 (Mahadevan et al., 1991). If *Mad2* null cells proceed through the cell cycle during nocodazole treatment, they should have a similar (or higher) S phase index than wt cells. Embryos were grown on chambered microscope slides to E5.5, treated with 2.5 μM nocodazole for 6 hr and with BrdU during the final 3 hr, digested with collagenase (to remove the basal lamina and promote antibody access to the ICM), and then fixed and stained (Figure 5). Wild type and heterozygous embryos treated with nocodazole showed a large increase in the number of phospho-Histone H3 positive cells as compared to untreated embryos (Figures 5F and 5G). In contrast, no increase in the number of phospho-Histone H3 positive cells was observed in nocodazole-treated *Mad2* null embryos (Figure 5H). This confirms data obtained with disaggregated cells (Figures 5A–5D). Significantly, the fraction of BrdU-positive cells was similar in wt and *Mad2* null embryos (about 50%), indicating that similar numbers of cells were actively synthesizing DNA. Thus, *Mad2* null cells are passing through the cell cycle at E5.5 even though they fail to arrest in response to nocodazole treatment. We conclude that the disruption of *Mad2* in mice inactivates the mitotic spindle assembly checkpoint just as it does in yeast (Li and Murrau, 1991; He et al., 1997). In yeast, *MAD2* deletion causes an alteration in the regulation rather than the mechanics of mitosis. We have been unable to investigate this in detail in early mouse embryos, but we do see evidence of correct spindle assembly and aligned chromosomes in *Mad2*$^{-/-}$ cells even past E5.5 (Figure 6). Thus, the mechanics of chromosome segregation appear to be more or less normal.

Chromosome Missegregation in *Mad2* Null Cells

Why do *Mad2* null mouse cells die in utero and in culture at E6.5–E7.5? One possibility is that the loss of checkpoint function results in a gross failure of chromosome segregation so that one daughter cell ends up with little or no DNA and dies. This type of missegregation is observed in yeast mutants such as *ndc10* and *esp1* (McGrew et al., 1992; Goh and Kilmartin, 1993). An alternate possibility is that there are subtle defects in mitosis and that the missegregation of one or a small number of chromosomes induces cell death. To investigate the occurrence of chromosome missegregation in mice, E6.5–E7.5 embryos from intercrosses of wt and *Mad2*$^{+/-}$ animals were sectioned in utero, the chromosomes were stained with Hoechst 33342, and the sections examined by laser confocal microscopy (Figure 6).

In wt embryos, the total number of mitotic cells more than doubled between E6.5 and E7.5 (Figure 6A, dark bars). In virtually all anaphase cells, mitosis appeared normal (>97% of mitotic cells), with chromosomes in two distinct groups clustered around the spindle poles. In contrast, in histologically abnormal embryos from heterozygous intercrosses (presumptive *Mad2* nulls; see above), mitosis appeared to have gone awry (Figures 6A and 6B, light bars). By E6.5, the total number of

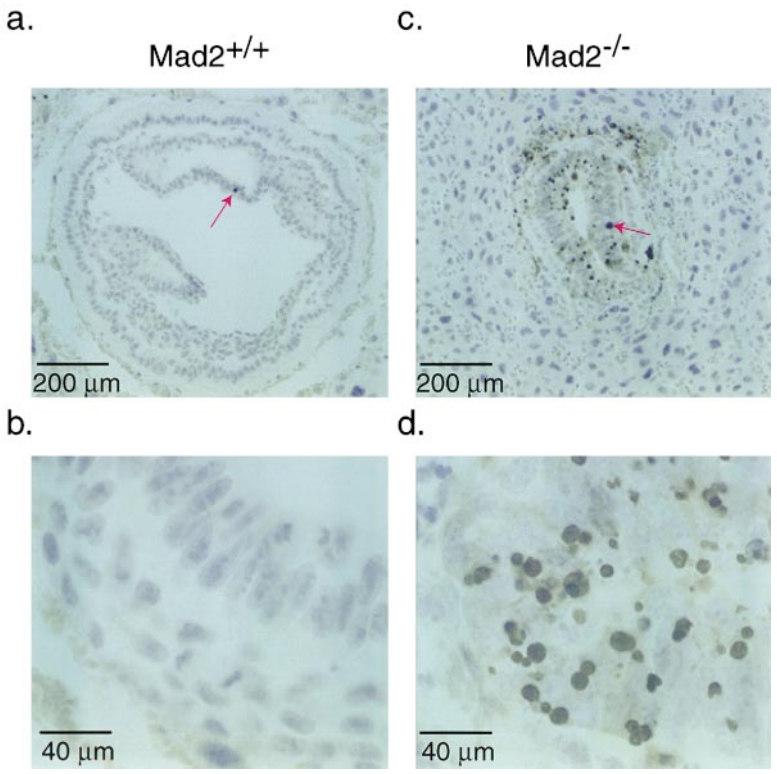

Figure 4. Analysis of Apoptosis in *Mad2*$^{-/-}$ Embryos In Utero

TUNEL staining of transversely sectioned E7.0 embryos in utero at low (A and C) and high (B and D) magnifications. Arrows point to TUNEL-positive apoptotic cells. The genotyping of embryonic sections was performed on samples collected by laser capture microscopy and was often complicated by the contamination of embryonic tissue by maternal tissue. We therefore relied on morphological methods to genotype the majority of embryos. However, the mutant embryos shown in this figure were unambiguously genotyped by PCR. Wild-type embryos were derived from wt intercrosses (and therefore did not require genotyping). H & E analysis showed that embryos unambiguously genotyped as homozygous *Mad2* nulls were small and abnormal in gross morphology as compared to wt controls, and displayed evidence of aberrant mitosis (Figure 6). Both of these phenotypes were seen in only about a fifth of the embryos from *Mad2*$^{+/-}$ intercrosses, and never in wild-type crosses, linking them to the *Mad2* null genotype (Table 1). We therefore classified as presumptive *Mad2* nulls all those embryos that were small and exhibited abnormal histology.

mitotic cells was markedly reduced and remained relatively unchanged through E7.5. Strikingly, about 25% of mitotic cells in abnormal embryos contained one or more chromosomes that were separated from the bulk of the pole-proximal DNA (Figures 6C and 6D). The high incidence of these lagging chromosomes suggests that anaphase is proceeding in *Mad2* null cells in the absence of complete chromosome–microtubule attachment. This type of missegregation is consistent with the failure of *Mad2* null cells to arrest in response to spindle damage induced by microtubule depolymerization (Figure 5).

Even though mutant embryos contain a high proportion of cells with lagging chromosomes, it is important to note that at least until E6.5, mitotic spindles still assemble and the bulk of the DNA is evenly divided between daughter cells (Figures 6E and 6F). We have observed no difference between the spindles of wt and *Mad2* null cells, nor have we observed cells with obviously subgenomic complements of DNA, in contrast to what is seen in budding yeast that carry mutations in essential kinetochore proteins (Goh and Kilmartin, 1993). We conclude from these observations that cells in which the Mad2-dependent checkpoint is abolished (as evidenced by in vitro challenges with nocodazole) are capable of assembling largely normal spindles and of correctly segregating the bulk of their DNA.

Discussion

We have shown that *Mad2*$^{-/-}$ embryonic mouse cells at E5.5, like *mad2* yeast, assemble spindles and undergo mitosis but do not arrest in response to microtubule depolymerization. The most striking difference between *Mad2* in higher and lower eukaryotes is that *Mad2* is essential in mouse cells after E6.5 but is dispensable for normal cell division in yeast (Li and Murray, 1991; He et al., 1997). In utero, *Mad2* null mouse embryos undergo programmed cell death after the initiation of gastrulation (E6.5), a particularly active period of cell division characterized by very short cell cycles (as short as 4–6 hr for some cell types) (Snow, 1977; Hogan et al., 1994). In culture, the death of *Mad2*$^{-/-}$ cells is restricted to the rapidly dividing cells of the inner cell mass. The postmitotic and highly polyploid trophoblast giant cells survive, arguing that Mad2 is required selectively in cells undergoing mitosis.

Although we have found that *Mad2*$^{-/-}$ animals derived from either of two independent lines are inviable, a number of animal studies remain to be done. One issue requiring further investigation is that fewer *Mad2*$^{-/-}$ embryos are recoverable, even at the earliest times after conception, than one would expect. It is possible that this reflects some probability of catastrophic chromosome missegregation prior to E3.5, the time at which embryos are harvested. Alternatively, *Mad2*$^{-/-}$ embryos may have a partially penetrant early embryonic defect unrelated to mitosis. Also requiring follow-up is preliminary histology that shows atypical germinal center morphology in the spleens of *Mad2*$^{+/-}$ animals. We are currently looking for cell cycle defects and tumors in highly proliferative hematopoietic lineages.

Mouse Mad2 Is Required for Checkpoint-Dependent Arrest

The observation that Mad2 binds to Mad1 (Chen et al., 1998, 1999; Jin et al., 1998) and to Cdc20-APC (Li et al., 1997; Fang et al., 1998; Hwang et al., 1998; Kim et al., 1998; Wassmann and Benezra, 1998) in both animal

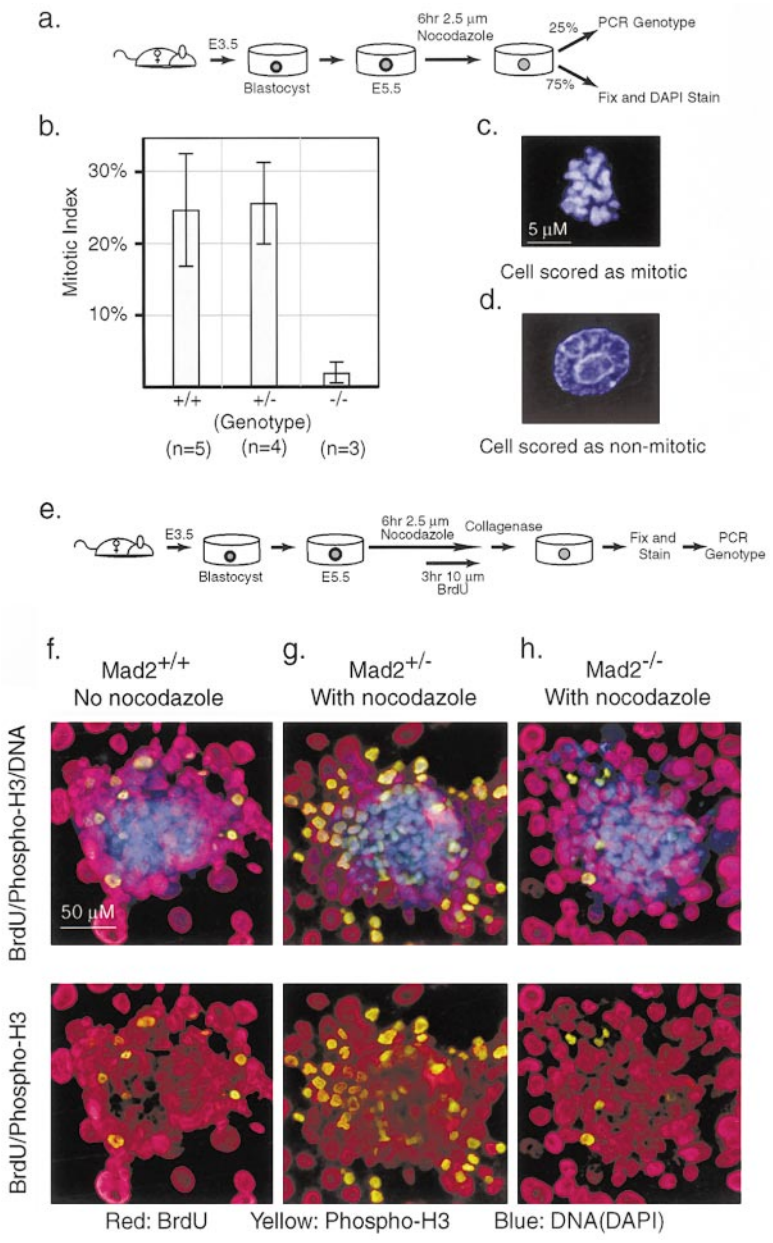

Figure 5. Analysis of Checkpoint Response in Cultured *Mad2*$^{-/-}$ Embryos

(A) Experimental outline. Blastocysts harvested at E3.5 from intercrosses of *Mad2*$^{+/-}$ mice were cultured in vitro to E5.5, treated with 2.5 μM nocodazole for 6 hr and analyzed for mitotic arrest.

(B–D) Quantitative analysis of mitotic arrest in disaggregated embryos. (B) Mitotic index for embryos of various genotypes. "n" indicates number of embryos analyzed. Error bars represent one standard deviation. The total number of DAPI-stained cells per embryo ranged from 17 to 113, with no statistically significant differences among various genotypes. The mitotic index was determined by counting cells with condensed (C) and noncondensed chromosomes (D).

(E–H) Analysis of S phase and mitotic index in whole mounts. (E) Experimental outline. Blastocysts harvested at E3.5 from intercrosses of *Mad2*$^{+/-}$ mice were cultured in vitro to E5.5, treated with 2.5 μM nocodazole for 6 hr and 10 μM BrdU for 3hr, and then briefly digested with collagenase to promote antibody access to the inner cell mass. After imaging, embryos were genotyped by PCR. (F–H) Embryos were processed for indirect immunofluorescence using anti-BrdU (red) and anti-phospho-Histone-H3 (yellow) antibodies. Each embryo is shown both with DAPI staining (above) and without (below). No difference was observed in the incidence of mitotic arrest between wt and heterozygous embryos.

cells and yeast implies that Mad2 is part of a signaling pathway conserved among higher and lower eukaryotes. However, the presence in animal cells of multiple Mad2-like proteins (Li and Benezra, 1996) and the discovery that Mad2 may bind to proteins as diverse as the insulin receptor (O'Neill et al., 1997) and metalloprotease disintegrins (Nelson et al., 1999) makes it essential to obtain genetic data about Mad2 function. By manipulating E5.5 embryonic cells in culture, we have examined the effect of deleting *Mad2* on the cell cycle arrest induced by disrupting microtubules of the mitotic spindle. We find that that the mitotic index of *Mad2*$^{-/-}$ embryonic cells is virtually identical before and after treatment with nocodazole. In contrast, the mitotic index of wild-type embryonic cells rises nearly 10-fold in response to a 6 hr nocodazole treatment. Thus, spindle damage provokes a cell-cycle arrest in wild-type embryonic cells, but not in *Mad2*$^{-/-}$ cells. We conclude that Mad2 is required for the spindle assembly checkpoint in mouse cells as it is in yeast (Li and Murray, 1991; He et al., 1997). These data are consistent with previously reported injection/electroporation experiments performed with PtK1 (Gorbsky et al., 1998) and HeLa cells (Li and Benezra, 1996), in which anti-Mad2 antibodies abolish nocodazole-induced mitotic arrest and cause premature mitotic exit.

Mad2 Null Cells Have High Rates of Chromosome Loss

In this paper, we provide genetic evidence in mammalian cells that the spindle assembly checkpoint is required for accurate chromosome segregation in the absence of spindle damage. The deletion of mouse *Mad2* appears to cause the rate of chromosome missegregation to rise

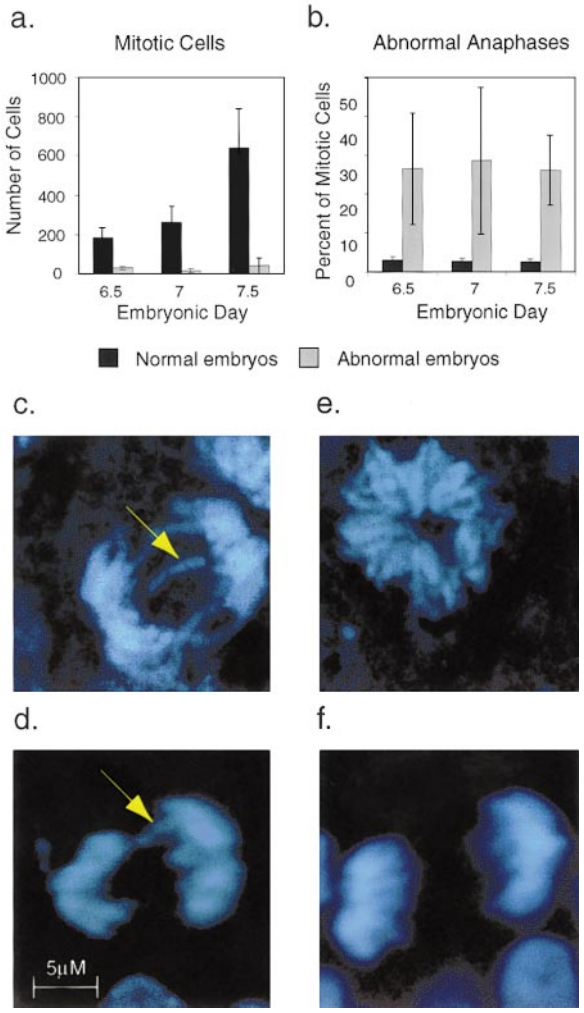

Figure 6. Analysis of Chromosome Missegregation in *Mad2*$^{-/-}$ Cells

Analysis of chromosome segregation in utero in E6.5–E7.5 embryos. Embryos were fixed, embedded, sectioned, stained with Hoechst 33342, and examined by confocal microscopy. Abnormal embryos, with a presumptive *Mad2*$^{-/-}$ genotype, were distinguished from presumptive wt and *Mad2*$^{+/-}$ embryos by overall size and morphology in H & E stained sections (Figure 4 legend). Each data point is derived from an analysis of at least three embryos.

(A) Comparison of the total number of mitotic cells in abnormal and normal embryos. Cells were scored as mitotic based on chromosome condensation. Error bars represent one standard deviation.

(B) Quantitative analysis of chromosome missegregation. The fraction of mitotic cells that exhibited a defect in segregation, such as a lagging chromosome (see C and D) is shown.

(C–F) Spindle morphologies in cells from presumptive *Mad2* null embryos at E6.5. A significant fraction of anaphase cells contained one or more chromosomes clearly separated from the bulk of DNA clustered at the poles (C and D). These lagging chromosomes are indicated by arrows. Other cells had apparently normal spindle morphologies (E and F).

dramatically. In many cases, we see evidence that one chromosome is left behind at the metaphase plate when the majority of chromosomes have moved to the poles. However, spindles do form and the great majority of chromosomes are correctly aligned and properly segregated. It seems very likely that the high proportion of lagging chromosomes reflects a failure of *Mad2*$^{-/-}$ cells to delay anaphase until all chromosomes have achieved proper bivalent attachment to spindle microtubules. We conclude that the checkpoint is not necessary for spindle assembly per se, but is required to provide sufficient time for the completion of the stochastic process of chromosome capture. This conclusion is consistent with anti-Mad2 microinjection experiments in HeLa cells (Gorbsky et al., 1998), and with the finding that the expression of a dominant negative fragment of mouse *Bub1* shortens the average time that a cell spends in mitosis (Taylor and McKeon, 1997).

Technical difficulties prevent us from scoring chromosome missegregation prior to E5.5 but there is no evidence that early *Mad2*$^{-/-}$ embryos have reduced rates of growth or altered S phase and mitotic indexes. Thus, the rate of chromosome missegregation appears to rise dramatically at E6.5. Why does missegregation only become apparent this late in development? One possibility is that in mice, as in *Xenopus*, the checkpoint does not function (and is not required) in the very early embryonic cell cycles (Chen et al., 1996). A second possibility is that maternal transcripts provide sufficient Mad2 for early divisions but that the maternal store is eventually exhausted. However, several studies have shown that the vast majority of RNA in E3.5 and later embryos arises from zygotic transcription and that maternal mRNAs are largely gone (Bachvarova and De Leon, 1980; Nothias et al., 1995). Exhaustion of maternal *Mad2* mRNA therefore seems an unlikely explanation for the late onset of a phenotype. A final possibility is that the checkpoint only becomes critical at about the time of gastrulation, when embryos enter a period of rapid cell division (Snow, 1977; Hogan et al., 1994). We favor this final explanation because it links changes in cell cycle timing to an increased reliance on checkpoint-imposed mitotic delay.

Death in *Mad2* Null Cells

What is the cause of apoptosis in *Mad2* null cells? While we cannot exclude the possibility that cell death is unrelated to the function of Mad2 in mitosis, the most attractive possibility is that missegregated chromosomes themselves trigger programmed cell death. Apoptosis occurs across the entire embryo at E6.5–E7.5, the point in development at which the cell cycle is reduced to as few as 4–6 hr (Snow, 1977; Hogan et al., 1994) making correct chromosome segregation more dependent on the spindle assembly checkpoint. We propose that cells lacking Mad2 at E6.5 exit mitosis early, causing DNA damage that induces apoptosis, perhaps via p53 (Basu et al., 1998; Lanni and Jacks, 1998). We are currently testing this idea by determining whether the disruption of p53 increases the survival of Mad2$^{-/-}$ embryos. The finding that Mad2 deletion promotes apoptosis contrasts with an earlier observation that apoptosis induced by treating HeLa cells with nocodazole is reduced by the overexpression of dominant negative fragments of Bub1 (Taylor and McKeon, 1997). Whether this reflects a difference between Mad2 and Bub1 or between embryonic cells and a transformed cell line is not known.

Mitotic Checkpoints in Yeast and Metazoans

The remarkable fidelity of chromosome segregation is dependent in part on the operation of mitotic checkpoints (Hoyt et al., 1991; Li and Murray, 1991; Li and

Nicklas, 1995). In the classical view (Hartwell and Weinert, 1989), checkpoints are nonessential and their inactivation only has an effect on those few cells in which mitosis goes awry. However, genetic analysis of *Mad2* in mouse, *bub1* in *Drosophila* (Basu et al., 1999), and *mad1* in *C. elegans* (Kitagawa and Rose, 1999) indicates that mitotic checkpoint genes are essential for cell viability in higher eukaryotes. This might appear to represent a fundamental difference between higher and lower eukaryotes, but real-time observations of mitosis in PtK1 cells suggest a unifying model (Rieder et al., 1994; Gorbsky et al., 1998). The duration of mitosis in PtK1 cells (from nuclear envelope breakdown to the initiation of anaphase) varies from about 30 min to over 3 hr. Regardless of the total time required for mitosis, anaphase starts almost exactly 23 min after the final chromosome makes proper attachment to the microtubules of the mitotic spindle (Rieder et al., 1994). In cells microinjected with anti-Mad2 antibodies, anaphase starts an average of 15 min after nuclear envelope breakdown, regardless of the status of spindle assembly (Gorbsky et al., 1998). Thus, the duration of mitosis in PtK1 cells appears to depend on both intrinsic timing (which accounts for the first about 15 min of mitosis) and on checkpoint-imposed delays (which provide whatever additional time is required to complete spindle assembly).

We can easily imagine that differences in the intrinsic rate of cell cycle progression or the rate of chromosome–microtubule capture could alter the importance of checkpoint-imposed delays, even in the absence of exogenous spindle damage. Thus, the absolute requirement for the checkpoint in higher eukaryotes, but not in budding yeast, might reflect a faster intrinsic clock and slower rate of chromosome–microtubule attachment and the presence of cell death pathways that are sensitive to chromosome damage. The observation that the deletion of *S. pombe Bub1* causes widespread chromosome missegregation demonstrates that checkpoints are required for accurate mitosis under normal growth conditions, but that fission yeast can tolerate high rates of chromosome loss (Bernard et al., 1998).

Mitotic Checkpoints, Apoptosis, and Tumorigenesis

The connection between checkpoints, aneuploidy, and cancer has several intriguing facets. In addition to the long-standing observation that the vast majority of tumor cells are aneuploid (Mitelman, 1971; Hartwell and Kastan, 1994; Kinzler and Vogelstein, 1996), it has recently been shown that cells from human colorectal cancers have a continuous high rate of chromosome loss and gain (giving rise to a chromosome instability or CIN phenotype) (Lengauer et al., 1997). Some human lung and colorectal cancers have also been shown to harbor mutations in the spindle assembly checkpoint genes *Bub1* and *Mad1* (Cahill et al., 1998; Nomoto et al., 1999). Checkpoint lesions that increase the rate of chromosome missegregation have the potential to be tumor promoting by acting as mutators that cause wild-type tumor suppressor alleles to be lost and recessive mutations to be uncovered. However, if chromosome missegregation triggers cell death, as suggested by the findings in this paper, it may be necessary for cells to acquire antiapoptotic mutations to exhibit a CIN phenotype. If so, we might expect chromosome instability to occur not during the earliest stages of tumorigenesis, but rather at later stages when antiapoptotic oncogenic lesions have already accumulated. Using various recombinant mouse strains it should be possible to test this idea.

Experimental Procedures

Cloning and Sequence Analysis of Murine *Mad2*

Mouse *Mad2* genomic DNA was isolated from a 129/Sv genomic library (Stratagene) using bp 5–102 of rat *Mad2* cDNA (dbEST ID 294792). Sequencing three of the 19 clones yielded *Mad2a*, *b*, and *d* (Figure 1). A separate screen yielded *Mad2c* (Figure 1). To determine which locus contributes to *Mad2* mRNA, rat *Mad2* cDNA was used to probe a mouse E10.5 cDNA library (Novagene). 23 of 28 clones contained cDNAs encoded by *Mad2a*; 2 of these contained an alternative 3′ noncoding UTR; 5 cDNAs encoded either truncated *Mad2* genes or genes unrelated to *Mad2*.

Generating *Mad2*$^{+/-}$ Mice

A *Mad2* deletion was generated by replacing the 5 kb genomic fragment encoding *Mad2* (from initiating methionine to stop codon) with a PGK-neomycin resistance cassette (Figure 2A; further details are available upon request). Gene targeting of *Mad2* in 129/Sv-derived D3 embryonic stem cells (Gossler et al., 1986) was carried out using positive-negative selection (Capecchi, 1989). Chimeric mice were created by injecting two independently derived *Mad2a*-targeted ES cell lines into C57BL/6 blastocysts generated by superovulation. Chimeras were crossed to BL/6 wt animals to generate founder lines.

Growth and Analysis of Mouse Embryos

Embryo Culture

E3.5 blastocysts from natural matings were harvested into 96-well plates or gelatinized chambered microscopy slides (Lab-Tek). Acidic Tyrode solution was used to remove the zona pellucida of blastocysts grown on slides (Hogan et al., 1994). Embryos were cultured without LIF in DMEM, 15% fetal bovine serum for a total of 2–5 days and examined by phase contrast microscopy prior to genotyping by PCR.

Whole Mounts

Blastocysts harvested at E3.5 were grown in culture on chambered microscope slides to E5.5, digested with 0.04% collagenase 3 (Worthington) for 20 min at 37°C to remove the basal lamina, and fixed for 10 min with 4% paraformaldehyde (EM Science). Cells were permeabilized with 0.5% Triton X-100 for 10 min, the DNA denatured and the embryos blocked (Leonhardt et al., 1992) and reacted with anti-BrdU antibodies (Becton Dickinson, 1:3.5 dilution) and anti-phospho-Histone H3 antibodies (Upstate BioTechnology, 1:400 dilution) for 1 hr at 37°C, followed by 45 min with anti-rabbit or anti-mouse secondary antibodies (Jackson ImmunoResearch). Embryos were viewed and photographed on a Zeiss-DeltaVision deconvolution microscope (Applied Precision), and then genotyped by PCR.

Disaggregated Embryonic Cells

E3.5 blastocysts were grown to E5.5–E6.5 in 96-well plates, trypsinized, and dried onto glass coverslips in 4% paraformaldehyde (see Figure 5A).

Analysis of Embryos In Utero

Decidua of E5.5 embryos were surgically removed, fixed in 4% paraformaldehyde at 4°C overnight, and embedded in paraffin blocks. 8 μm sections were incubated on slides at 42°C overnight and then deparaffinized, rehydrated, and mounted in 1 ng/ml Hoechst 33342 in 1 mg/ml p-phenylenedamine, 0.1× PBS, and 80% glycerol. Slides were examined by laser confocal microscopy (LSM510, Zeiss).

TUNEL reactions were performed on deparaffinized and dehydrated embryo sections following a modified version of standard TUNEL protocol (Gavrieli et al., 1992). Following microscopic examination, embryos were genotyped by PCR analysis of laser-captured embryonic tissue.

PCR Genotyping

Mice were genotyped using primers for PCR-A and PCR-C (Figure 2A) on tails digested overnight in lysis buffer (1 mg/ml proteinase K, 67 mM Tris [pH 8.8], 17 mM ammonium sulfate, 6.5 mM $MgCl_2$, 1% 2-mercaptoethanol, and 0.5% Triton X-100). Embryos grown in culture were digested in lysis buffer and phenol-chloroform extracted, chloroform extracted, and ethanol precipitated. One-half of each embryo DNA preparation was analyzed with PCR-B primers and the other with PCR-C primers. The first round PCR was then reamplified using nested primers. Tissue from paraffin-embedded embryo sections was collected by laser capture, digested, and analyzed as described above for embryos. Primer sequences and reaction conditions are available upon request.

Acknowledgments

V. L. performed the in utero analysis of missegregation and apoptosis phenotypes in *Mad2* null embryos. We thank R. Kirchweger for her contributions; B. Panning, K. Manova, H. Zhang, D. Baltimore, T. Jacks, J. Harrison, E. Brown, and J. Copeland for assistance; C. Shamu, A. Amon, I. Russell, and members of the Benezra and Sorger labs for critical reading of the manuscript. This work was supported by the Searle Scholars Fund, Merck and Co., R01 CA84179 (P. K. S.), R01 GM 54601(R. B.), and BD18587/98, from PRAXISXXI, Portugal (V. L.).

Received January 27, 2000; revised April 27, 2000.

References

Alexandru, G., Zachariae, W., Schleiffer, A., and Nasmyth, K. (1999). Sister chromatid separation and chromosome re-duplication are regulated by different mechanisms in response to spindle damage. EMBO J. *18*, 2707–2721.

Bachvarova, R., and De Leon, V. (1980). Polyadenylated RNA of mouse ova and loss of maternal RNA in early development. Dev. Biol. *74*, 1–8.

Basu, J., Logarinho, E., Herrmann, S., Bousbaa, H., Li, Z., Chan, G.K., Yen, T.J., Sunkel, C.E., and Goldberg, M.L. (1998). Localization of the Drosophila checkpoint control protein Bub3 to the kinetochore requires Bub1 but not Zw10 or Rod. Chromosoma *107*, 376–385.

Basu, J., Bousbaa, H., Logarinho, E., Li, Z., Williams, B.C., Lopes, C., Sunkel, C.E., and Goldberg, M.L. (1999). Mutations in the essential spindle checkpoint gene bub1 cause chromosome missegregation and fail to block apoptosis in Drosophila. J. Cell Biol. *146*, 13–28.

Bernard, P., Hardwick, K., and Javerzat, J.P. (1998). Fission yeast bub1 is a mitotic centromere protein essential for the spindle checkpoint and the preservation of correct ploidy through mitosis. J. Cell Biol. *143*, 1775–1787.

Cahill, D.P., Lengauer, C., Yu, J., Riggins, G.J., Willson, J.K., Markowitz, S.D., Kinzler, K.W., and Vogelstein, B. (1998). Mutations of mitotic checkpoint genes in human cancers. Nature *392*, 300–303.

Capecchi, M.R. (1989). Altering the genome by homologous recombination. Science *244*, 1288–1292.

Chan, G.K., Schaar, B.T., and Yen, T.J. (1998). Characterization of the kinetochore binding domain of CENP-E reveals interactions with the kinetochore proteins CENP-F and hBUBR1. J. Cell Biol. *143*, 49–63.

Chan, G.K., Jablonski, S.A., Sudakin, V., Hittle, J.C., and Yen, T.J. (1999). Human BUBR1 is a mitotic checkpoint kinase that monitors CENP-E functions at kinetochores and binds the cyclosome/APC. J. Cell Biol. *146*, 941–954.

Chen, R.H., Waters, J.C., Salmon, E.D., and Murray, A.W. (1996). Association of spindle assembly checkpoint component XMAD2 with unattached kinetochores. Science *274*, 242–246.

Chen, R.H., Shevchenko, A., Mann, M., and Murray, A.W. (1998). Spindle checkpoint protein Xmad1 recruits Xmad2 to unattached kinetochores. J. Cell Biol. *143*, 283–295.

Chen, R.H., Brady, D.M., Smith, D., Murray, A.W., and Hardwick, K.G. (1999). The spindle checkpoint of budding yeast depends on a tight complex between the Mad1 and Mad2 proteins. Mol. Biol. Cell *10*, 2607–2618.

Clute, P., and Pines, J. (1999). Temporal and spatial control of cyclin B1 destruction in metaphase. Nat. Cell Biol. *1*, 82–87.

Cohen-Fix, O., Peters, J.M., Kirschner, M.W., and Koshland, D. (1996). Anaphase initiation in Saccharomyces cerevisiae is controlled by the APC-dependent degradation of the anaphase inhibitor Pds1p. Genes Dev. *10*, 3081–3093.

Fang, G., Yu, H., and Kirschner, M.W. (1998). The checkpoint protein MAD2 and the mitotic regulator CDC20 form a ternary complex with the anaphase-promoting complex to control anaphase initiation. Genes Dev. *12*, 1871–1883.

Fraschini, R., Formenti, E., Lucchini, G., and Piatti, S. (1999). Budding yeast Bub2 is localized at spindle pole bodies and activates the mitotic checkpoint via a different pathway from Mad2. J. Cell Biol. *145*, 979–991.

Gavrieli, Y., Sherman, Y., and Ben-Sasson, S.A. (1992). Identification of programmed cell death in situ via specific labeling of nuclear DNA fragmentation. J. Cell Biol. *119*, 493–501.

Goh, P.Y., and Kilmartin, J.V. (1993). NDC10: a gene involved in chromosome segregation in Saccharomyces cerevisiae. J. Cell Biol. *121*, 503–512.

Gorbsky, G.J., Chen, R.H., and Murray, A.W. (1998). Microinjection of antibody to Mad2 protein into mammalian cells in mitosis induces premature anaphase. J. Cell Biol. *141*, 1193–1205.

Gossler, A., Doetschman, T., Korn, R., Serfling, E., and Kemler, R. (1986). Transgenesis by means of blastocyst-derived embryonic stem cell lines. Proc. Natl. Acad. Sci. USA *83*, 9065–9069.

Hardwick, K.G., Weiss, E., Luca, F.C., Winey, M., and Murray, A.W. (1996). Activation of the budding yeast spindle assembly checkpoint without mitotic spindle disruption. Science *273*, 953–956.

Hardwick, K.G., Johnston, R.C., Smith, D.L., and Murray, A.W. (2000). MAD3 encodes a novel component of the spindle checkpoint which interacts with bub3p, cdc20p, and mad2p. J. Cell Biol. *148*, 871–882.

Hartwell, L.H., and Kastan, M.B. (1994). Cell cycle control and cancer. Science *266*, 1821–1828.

Hartwell, L.H., and Weinert, T.A. (1989). Checkpoints: controls that ensure the order of cell cycle events. Science *246*, 629–634.

Hartwell, L., Dutcher, S., Wood, J., and Garvik, B. (1982). The fidelity of mitotic chromosome reproduction in *S. cerevisiae*. Rec. Adv. Yeast Mol. Biol. *1*, 28.

He, X., Patterson, T.E., and Sazer, S. (1997). The Schizosaccharomyces pombe spindle checkpoint protein mad2p blocks anaphase and genetically interacts with the anaphase-promoting complex. Proc. Natl. Acad. Sci. USA *94*, 7965–7970.

Hogan, B., Beddington, R., Constantini, F., and Lacy, E. (1994). Manipulating the Mouse Embryo, 2nd Edition (Cold Spring Harbor, NY: Cold Spring Harbor Laboratory Press).

Hoyt, M.A., Totis, L., and Roberts, B.T. (1991). S. cerevisiae genes required for cell cycle arrest in response to loss of microtubule function. Cell *66*, 507–517.

Hwang, L.H., Lau, L.F., Smith, D.L., Mistrot, C.A., Hardwick, K.G., Hwang, E.S., Amon, A., and Murray, A.W. (1998). Budding yeast Cdc20: a target of the spindle checkpoint. Science *279*, 1041–1044. Erratum: Science *280*(5368), 1998.

Jin, D.Y., Spencer, F., and Jeang, K.T. (1998). Human T cell leukemia virus type 1 oncoprotein Tax targets the human mitotic checkpoint protein MAD1. Cell *93*, 81–91.

Jordan, M.A., Wendell, K., Gardiner, S., Derry, W.B., Copp, H., and Wilson, L. (1996). Mitotic block induced in HeLa cells by low concentrations of paclitaxel (Taxol) results in abnormal mitotic exit and apoptotic cell death. Cancer Res. *56*, 816–825.

Kim, S.H., Lin, D.P., Matsumoto, S., Kitazono, A., and Matsumoto, T. (1998). Fission yeast Slp1: an effector of the Mad2-dependent spindle checkpoint. Science *279*, 1045–1047.

Kinzler, K.W., and Vogelstein, B. (1996). Lessons from hereditary colorectal cancer. Cell *87*, 159–170.

Kitagawa, R., and Rose, A.M. (1999). Components of the spindle-assembly checkpoint are essential in Caenorhabditis elegans. Nat. Cell Biol. *1*, 514–521.

Lanni, J.S., and Jacks, T. (1998). Characterization of the p53-dependent postmitotic checkpoint following spindle disruption. Mol. Cell. Biol. *18*, 1055–1064.

Lengauer, C., Kinzler, K.W., and Vogelstein, B. (1997). Genetic instability in colorectal cancers. Nature *386*, 623–627.

Leonhardt, H., Page, A.W., Weier, H.U., and Bestor, T.H. (1992). A targeting sequence directs DNA methyltransferase to sites of DNA replication in mammalian nuclei. Cell *71*, 865–873.

Li, R. (1999). Bifurcation of the mitotic checkpoint pathway in budding yeast. Proc. Natl. Acad. Sci. USA *96*, 4989–4994.

Li, Y., and Benezra, R. (1996). Identification of a human mitotic checkpoint gene: hsMAD2. Science *274*, 246–248.

Li, R., and Murray, A.W. (1991). Feedback control of mitosis in budding yeast. Cell *66*, 519–531. Erratum: Cell, *79*(2).

Li, X., and Nicklas, R.B. (1995). Mitotic forces control a cell-cycle checkpoint. Nature *373*, 630–632.

Li, Y., Gorbea, C., Mahaffey, D., Rechsteiner, M., and Benezra, R. (1997). MAD2 associates with the cyclosome/anaphase-promoting complex and inhibits its activity. Proc. Natl. Acad. Sci. USA *94*, 12431–12436.

Mahadevan, L.C., Willis, A.C., and Barratt, M.J. (1991). Rapid histone H3 phosphorylation in response to growth factors, phorbol esters, okadaic acid, and protein synthesis inhibitors. Cell *65*, 775–783.

Martinez-Exposito, M.J., Kaplan, K.B., Copeland, J., and Sorger, P.K. (1999). Retention of the BUB3 checkpoint protein on lagging chromosomes. Proc. Natl. Acad. Sci. USA *96*, 8493–8498.

McGrew, J.T., Goetsch, L., Byers, B., and Baum, P. (1992). Requirement for ESP1 in the nuclear division of Saccharomyces cerevisiae. Mol. Biol. Cell *3*, 1443–1454.

Mitelman, F. (1971). The chromosomes of fifty primary Rous rat sarcomas. Hereditas *69*, 155–186.

Nelson, K.K., Schlondorff, J., and Blobel, C.P. (1999). Evidence for an interaction of the metalloprotease-disintegrin tumour necrosis factor alpha convertase (TACE) with mitotic arrest deficient 2 (MAD2), and of the metalloprotease-disintegrin MDC9 with a novel MAD2-related protein, MAD2beta. Biochem. J. *343 Pt 3*, 673–680.

Nomoto, S., Haruki, N., Takahashi, T., Masuda, A., Koshikawa, T., Fujii, Y., and Osada, H. (1999). Search for in vivo somatic mutations in the mitotic checkpoint gene, hMAD1, in human lung cancers. Oncogene *18*, 7180–7183.

Nothias, J.Y., Majumder, S., Kaneko, K.J., and DePamphilis, M.L. (1995). Regulation of gene expression at the beginning of mammalian development. J. Biol. Chem. *270*, 22077–22080.

O'Neill, T.J., Zhu, Y., and Gustafson, T.A. (1997). Interaction of MAD2 with the carboxyl terminus of the insulin receptor but not with the IGFIR. Evidence for release from the insulin receptor after activation. J. Biol. Chem. *272*, 10035–10040.

Rieder, C.L., Schultz, A., Cole, R., and Sluder, G. (1994). Anaphase onset in vertebrate somatic cells is controlled by a checkpoint that monitors sister kinetochore attachment to the spindle. J. Cell Biol. *127*, 1301–1310.

Rieder, C.L., Cole, R.W., Khodjakov, A., and Sluder, G. (1995). The checkpoint delaying anaphase in response to chromosome monoorientation is mediated by an inhibitory signal produced by unattached kinetochores. J. Cell. Biol. *130*, 941–948.

Rugh, R. (1990). Normal development of the mouse. In The Mouse (London: Oxford University Press), pp. 44–101.

Shirayama, M., Zachariae, W., Ciosk, R., and Nasmyth, K. (1998). The Polo-like kinase Cdc5p and the WD-repeat protein Cdc20p/fizzy are regulators and substrates of the anaphase promoting complex in Saccharomyces cerevisiae. EMBO J. *17*, 1336–1349.

Snow, M. (1977). Gastrulation in the mouse: growth and regionalization of the epiblast. J. Embryol. Exp. Morphol. *42*, 293–303.

Taylor, S.S., Ha, E., and McKeon, F. (1998). The human homologue of Bub3 is required for kinetochore localization of Bub1 and a Mad3/Bub1-related protein kinase. J. Cell Biol. *142*, 1–11.

Taylor, S.S., and McKeon, F. (1997). Kinetochore localization of murine Bub1 is required for normal mitotic timing and checkpoint response to spindle damage. Cell *89*, 727–735.

Visintin, R., Prinz, S., and Amon, A. (1997). CDC20 and CDH1: a family of substrate-specific activators of APC-dependent proteolysis. Science *278*, 460–463.

Wassmann, K., and Benezra, R. (1998). Mad2 transiently associates with an APC/p55Cdc complex during mitosis. Proc. Natl. Acad. Sci. USA *95*, 11193–11198.

Woods, C.M., Zhu, J., McQueney, P.A., Bollag, D., and Lazarides, E. (1995). Taxol-induced mitotic block triggers rapid onset of a p53-independent apoptotic pathway. Mol. Med. *1*, 506–526.

Yamamoto, A., Guacci, V., and Koshland, D. (1996). Pds1p is required for faithful execution of anaphase in the yeast, Saccharomyces cerevisiae. J. Cell Biol. *133*, 85–97.

GenBank Accession Numbers

The complete sequences of Mad2a–d have been deposited in GenBank with accession numbers AF261919, AF261920, AF261921, and AF259902, respectively.